Journal of the Optical Society of America B
OPTICAL PHYSICS

Nonlinear stabilization of high-energy and ultrashort pulses in passively modelocked lasers

SHAOKANG WANG,* BRIAN S. MARKS, AND CURTIS R. MENYUK

Department of Computer Science and Electrical Engineering, University of Maryland, Baltimore County, 1000 Hilltop Circle, Baltimore, Maryland 21250, USA
**Corresponding author: swan1@umbc.edu*

Received 30 August 2016; revised 25 October 2016; accepted 27 October 2016; posted 2 November 2016 (Doc. ID 274839); published 22 November 2016

The two most commonly used models for passively modelocked lasers with fast saturable absorbers are the Haus modelocking equation (HME) and the cubic-quintic modelocking equation (CQME). The HME predicts an instability threshold that is unrealistically pessimistic. We use singular perturbation theory to demonstrate that the CQME has a stable high-energy solution for an arbitrarily small but nonzero quintic contribution to the fast saturable absorber. As a consequence, we find that the CQME predicts the existence of stable modelocked pulses when the cubic nonlinearity is orders of magnitude larger than the value at which the HME predicts that modelocked pulses become unstable. Our results suggest a possible path to obtain high-energy and ultrashort pulses by fine tuning the higher-order nonlinear terms in the fast saturable absorber.

OCIS codes: (000.4430) Numerical approximation and analysis; (140.4050) Mode-locked lasers; (140.3425) Laser stabilization.

https://doi.org/10.1364/JOSAB.33.002596

1. INTRODUCTION

Over the past few decades, ultrashort optical pulses that are produced by passively modelocked lasers have been used in many fields [1,2]. The Haus modelocking equation (HME) is the most widely used model that has been successfully used to explore many of the qualitative features of passively modelocked lasers. However, the predictions from the HME for the instability thresholds are unrealistically pessimistic due to the unlimited third-order nonlinear gain [3–5]. Another model is the complex Ginzburg–Landau equation (CGLE), in which the modelocked solutions are referred to as dissipative solitons [6,7]. The CGLE includes a higher-order saturation to the nonlinear gain, which is unlimited in the HME. Computational studies have shown that this model predicts a large stable region in the parameter space in which modelocked pulses exist. However, the CGLE assumes an instantaneous gain that does not exist in any real laser. A more realistic model of passively modelocked lasers is the cubic–quintic modelocking equation (CQME) [8,9], which includes both higher-order saturable absorption, which is absent in the HME, and a slow saturable gain, which is absent in the CGLE. We write the CQME as

$$\frac{\partial u}{\partial z} = \left[-i\phi - \frac{l}{2} + \frac{g(|u|)}{2}\left(1 + \frac{1}{2\omega_g^2}\frac{\partial^2}{\partial t^2}\right) - \frac{i\beta''}{2}\frac{\partial^2}{\partial t^2} + i\gamma|u|^2\right]u + f_{\mathrm{sa}}(u)u, \tag{1}$$

where u is the complex field envelope, t is the retarded time, z is the propagation distance, ϕ is the phase rotation per unit length, l is the linear loss coefficient, $g(|u|)$ is the saturated gain, β'' is the group velocity dispersion coefficient, γ is the Kerr coefficient, ω_g is the gain bandwidth, and $f_{\mathrm{sa}}(|u|)$ is the fast saturable absorption

$$f_{\mathrm{sa}}(u) = \delta|u|^2 - \sigma|u|^4, \tag{2}$$

in which δ is the cubic coefficient of the fast saturable absorption, and σ is the quintic coefficient that provides a higher-order saturation to the unlimited third-order nonlinear gain [6,10,11]. Equation (1) becomes the HME when $\sigma = 0$. In this paper, we focus on the case in which the chromatic dispersion is anomalous with $\beta'' < 0$. We assumed that the gain response of the medium is much longer than the roundtrip time T_R, in which case the saturable gain becomes

$$g(|u|) = g_0/[1 + P_{\mathrm{av}}(|u|)/P_{\mathrm{sat}}], \tag{3}$$

where g_0 is the unsaturated gain, $P_{\mathrm{av}}(|u|)$ is the average power, and $P_{\mathrm{sat}} = \int_{-T_R/2}^{T_R/2} |u(t,z)|^2 \mathrm{d}t/T_R$ is the saturation power. It is conventional to write Eq. (1) without a phase rotation ϕ, in which case the modelocked pulse solution will have a constant phase rotation. For computational reasons, it is more convenient to work with equations whose modelocked pulse solution is strictly stationary. For this reason, we find the stationary modelocked solution $u(t)$ in parallel with ϕ, as described in [8].

In prior work [8], we computationally found the stable region in the (σ, δ) parameter space for Eq. (1), using a parameter set that corresponds to a soliton laser ($\beta'' < 0$). We found that for a range of σ values, two stable modelocked pulse solutions exist. There is a low-amplitude solution that coincides with the stable solution of the HME when $\sigma \to 0$ and is stable over a limited range of δ values. Additionally, there is a high-energy solution—which is referred to as the high-amplitude solution in [8]—that, for the values of σ that we explored, remains stable up to $\delta \approx 9.51$, which is about a factor of 280 greater than the HME's stability limit.

However, the work in [8] left open the question of what happens to the high-amplitude solution when $\sigma \to 0$. In this work, we complete the stability study of the CQME in the anomalous disperison regime by investigating in detail the limit of Eq. (1) when $\sigma \to 0$. Using singular perturbation theory, we will show that the high-amplitude solution persists regardless of how small σ becomes, as long as it is nonzero. We will also show that the energy of this solution increases as $\sigma \to 0$, suggesting a path toward obtaining high-energy, ultrashort solutions. Since any real modelocked laser system with a fast saturable absorber will have a quintic component, this result also shows that the HME cannot be relied upon to quantitatively determine the stability in real systems.

In Section 2, we briefly review the stability structure of the CQME for the parameter set that we consider. In Sections 3 and 4, we study the high-amplitude solution using singular perturbation theory [12], which enables us to find the solution to Eq. (1) when $\sigma \to 0$ and to determine its stability. The energy of this solution increases and its duration decreases as $\sigma \to 0$, but the range of δ values in which it is stable does not change significantly. In Section 5, we discuss how these solutions could be obtained experimentally.

2. REVISITING THE STABILITY OF THE CQME

We show the set of normalized parameters that we use in Table 1. These values are the same as in Table 1 of [8]; the value $\omega_g = \sqrt{10}/2$ reported there is an error.

We previously used boundary tracking algorithms [8,13] to find the stable regions of the regions of the CQME in the (σ, δ) parameter plane. We found that there is a parameter range in which a low-amplitude solution (LAS) and a high-amplitude solution (HAS) can coexist. The LAS continues to exist when $\sigma = 0$ and is stable over a limited range of δ values, $0.01 < \delta < 0.0348$ [3]. The solution corresponds to the stable, stationary solution of the HME. By contrast, the HME has no solution that corresponds to the HAS of the CQME. On the other hand, the region in the (σ, δ) plane in which the HAS exists and is stable far larger than the region for the LAS. We have found computationally that the HAS remains stable up to $\delta \approx 9.51$ when $\sigma \neq 0$—a factor 280 larger than the maximum value of δ for the LAS. The coexistence of the LAS and the HAS has recently been observed experimentally [14]. Moreover, the existence of the HAS explains the experimental observation that the stable region predicted by the HME is unrealistically pessimistic [8,9]. Thus, the HAS plays an important role in practice.

We previously found computationally that when δ is as large as 9.51, the HAS remains stable when σ is as small as 7×10^{-4} [8]. However, this study did not determine what happens to the HAS for a physically reasonable range of δ as $\sigma \to 0$. It was unclear whether a stable HAS continues to exist, becomes unstable, or disappears. In Sections 3 and 4, we will show that the HAS exists and remains stable for any nonzero σ as long as $\delta \lesssim 9.51$. At the same time, its energy increases and its duration decreases—opening up a potential path to obtain high-energy pulses.

Table 1. Normalized Values of Parameters

Parameter	g_0	l	γ	ω_g	β''	$T_R P_{\text{sat}}$
Value	0.4	0.2	4	$\sqrt{5}$	−2	1

3. STATIONARY PULSE AS $\sigma \to 0$

We previously found computationally that the HAS remains stable up to $\delta \approx 9.51$ when σ is as small as 7×10^{-4} [8]. However, the computational approach that we used to obtain Fig. 16 in [8] does not continue to work well for the HAS when $\sigma \to 0$ because the pulse becomes singular; its energy increases and its duration decreases. This behavior is visible in Fig. 1, where we see the variation of the peak amplitude A_0 and its FWHM duration as σ decreases. An alternative approach is therefore required to determine whether a modelocked pulse exists in this limit and—if it continues to exist—whether it is stable. We use singular perturbation theory to address these questions.

A. Dominant Balance

From Fig. 1, we infer for all values of δ that $A_0 \propto \sigma^{-1/2}$ and $\tau_0 \propto \sigma^{1/2}$ as $\sigma \to 0$. Based on this observation, we seek a stationary (equilibrium) solution of Eq. (1) that has the form

$$\phi_0 = \psi_0 \sigma^{-1}, \qquad u_0(t) = \sigma^{-1/2} a_0(\sigma^{-1/2} t). \tag{4}$$

For the stationary solution, we must have $da_0/dz = d\psi_0/dz = 0$. We will find that the equations that govern a_0 and ψ_0 become independent of σ in the limit $\sigma \to 0$, which allows us to determine them.

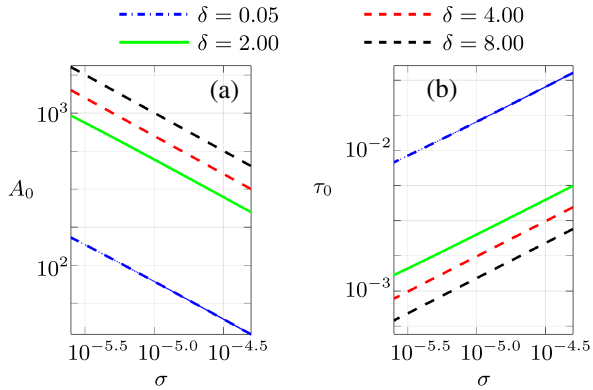

Fig. 1. (a) The peak amplitude A_0 and (b) the FWHM pulse duration τ_0 of the computational stationary pulse solution of the CQME as $\sigma \to 0$ and δ varies. The slopes of the curves equal −1/2 and 1/2 in (a) and (b), respectively.

We let $\tau = \sigma^{-1/2}t$, and we use a prime to denote derivatives with respect to τ, so that

$$\frac{\partial u_0}{\partial t} = a_0'\sigma^{-1}, \qquad \frac{\partial^2 u_0}{\partial t^2} = a_0''\sigma^{-3/2}. \tag{5}$$

We also find

$$g(|u|) = g_0/(1 + C_g\sigma^{-1/2}), \tag{6}$$

where $C_g = \int_{-\infty}^{\infty} |a_0(\tau)|^2 \mathrm{d}\tau/(P_{\mathrm{sat}}T_R)$. After substitution of Eq. (6) into Eq. (1), we find

$$(C_g\sigma + \sigma^{3/2})\frac{\partial a_0}{\partial z} = \frac{g_0 - l}{2}a_0\sigma^{3/2} - \frac{l}{2}C_g a_0\sigma + \sigma^{1/2}\left[\frac{g_0}{4\omega_g^2}a_0'' + f\right] + C_g f, \tag{7}$$

where $f = (\delta + i\gamma)|a_0|^2a_0 - |a_0|^4a_0 - i\psi a_0 - i\beta''a_0''/2$. As $\sigma \to 0$ and when $a(\tau) \neq 0$, the dominant balance of this system is

$$f = (\delta + i\gamma)|a_0|^2a_0 - |a_0|^4a_0 - i\psi_0 a_0 - \frac{i\beta''}{2}a_0'' = 0, \tag{8}$$

from which we solve for the asymptotic stationary solution $[a_0(\tau), \psi_0]$.

The balance of the dominant terms in Eq. (8) implies that, in the CQME of Eq. (1), as $\sigma \to 0$, the gain and the loss are balanced via the cubic term $\delta|a_0|^2a_0$ and the quintic term $\sigma|a_0|^4a_0$, while the saturated gain and the linear loss play no role in forming the stationary pulse. The remaining imaginary terms imply that the pulse envelope $a_0(\tau)$ is in general complex, i.e., a chirp is required to satisfy $f = 0$ in Eq. (8).

B. Asymptotic Stationary Pulse

We use the nonlinear root-finding method that is described in [8] to computationally solve Eq. (8). We consider the parameter set that is shown in Table 1. In Fig. 2, we show the profile of the asymptotic solution that we have found computationally, in which A_a is the peak amplitude of $a_0(\tau)$, $\tau_a = \tau_{a,\mathrm{FWHM}}/0.57$, where $\tau_{a,\mathrm{FWHM}}$ is the FWHM width of $a_0(\tau)$, and the chirp coefficient is given by

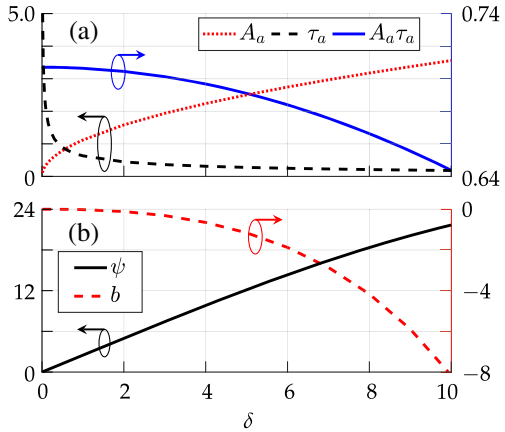

Fig. 2. (a) The peak amplitude A_a, the pulse width τ_a, and their product $A_a\tau_a$, (b) the rotation rate coefficient ψ, and the quadratic chirp coefficient b of the asymptotic stationary solution that is obtained by finding the root of f in Eq. (8).

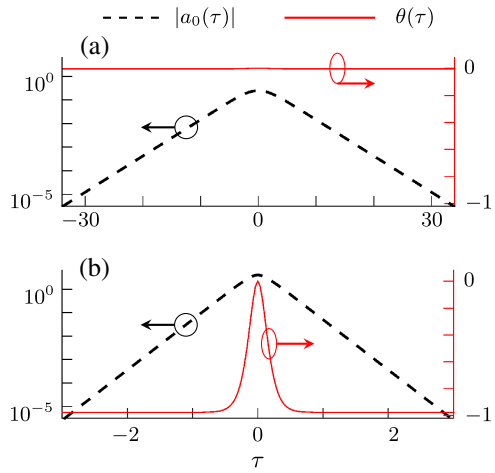

Fig. 3. Asymptotic stationary solution obtained by solving Eq. (8) with (a) $\delta = 0.05$ and (b) $\delta = 13.00$. Here, $\theta(\tau)$ is the phase change across the pulse in radians. Note that the scales of τ are different in the two subfigures.

$$b = \mathrm{Im}\frac{\int_{-\infty}^{\infty}\tau a_0^* a_0'\mathrm{d}\tau}{\int_{-\infty}^{\infty}\tau^2|a_0|^2\mathrm{d}\tau}. \tag{9}$$

As δ increases, the amplitude A_a increases while τ_a decreases, i.e., the asymptotic stationary pulse solution becomes increasingly taller and narrower. Meanwhile, we find that $A_a\tau_a \approx 1/\sqrt{2}$ when $\delta \approx 0$ and decreases as δ grows. Hence, the pulse shape is close to that of a nonlinear Schrödinger (NLS) equation soliton when δ is small, and it deviates from the NLS soliton profile as δ grows. In addition, when $\delta \approx 0$, the phase rotation rate coefficient ψ is close to 0, while the pulse is almost chirp-free. Then, as δ increases, we find that ψ increases, and the chirp across the pulse increases.

The amplitude of the asymptotic pulse solution that we have found is similar in shape to a hyperbolic-secant pulse, in which the wings of the pulse decay exponentially as $|t|$ increases. We show two examples of asymptotic pulses with $\delta = 0.05$ and $\delta = 13.00$ in Fig. 3, in which $\theta(\tau)$ is the phase change across the pulse, i.e., $a_0(\tau) = |a_0(\tau)|\exp[i\theta(\tau)]$. The variation of $\theta(\tau)$ increases significantly as δ increases, which is consistent with the change in the chirp parameter b that is shown in Fig. 2.

Afanasjev [15] has reported that the analytical pulse solutions of the CGLE becomes singular when both the linear gain and the quintic coefficient vanish, which is similar to our result. However, these analytical solutions are always unstable and cannot be used to model modelocked lasers [6–8].

4. STABILITY OF THE CQME AS $\sigma \to 0$

Next, we evaluate the stability of these stationary pulse solutions. We first linearize Eq. (7) about the stationary solution, and we determine the spectrum (eigenvalues) of this linearized equation. The spectrum that we find in this case is similar to the spectrum that appears in soliton perturbation theory [16,17]. There are two branches of eigenvalues that correspond to continuous wave perturbations, and there are four discrete modes that correspond to perturbations of the stationary solution's central time, central phase, amplitude, and central

frequency, and whose eigenvalues we will be denoted as λ_τ, λ_ϕ, λ_a, and λ_f, respectively. The solution is linearly stable if the real part of the two continuous branches are negative and the discrete eigenvalues λ_f and λ_a are both negative, while λ_τ and λ_ϕ remain at the origin due to time and phase invariance of Eq. (1).

A. Linearization

When we linearize Eq. (7), we can neglect the terms that are proportional to $\sigma^{3/2}$, as these terms tend to zero faster than terms proportional to σ^x with $x < 3/2$ as $\sigma \to 0$. If we add a perturbation Δa to the stationary pulse solution $a_0(\tau)$, and then linearize Eq. (7) about $a_0(\tau)$, we then obtain

$$\sigma\frac{\partial \Delta a}{\partial z} \approx -\frac{l}{2}\sigma\Delta a + \frac{\sigma^{1/2}}{C_g}\left(f_a + \frac{g_0}{4\omega_g^2}\Delta a''\right) + f_{a^*}, \tag{10}$$

where f_a is the derivative of f with respect to Δa,

$$f_a = (\delta + i\gamma)(2|a_0|^2\Delta a + a_0^2\Delta a^*) - i\beta''/2\Delta a'' - i\psi_0\Delta a - 3|a_0|^4\Delta a - 2|a_0|^2a_0^2\Delta a^*. \tag{11}$$

B. Continuous Waves

The stability condition for the continuous modes is $g(|u|) - l < 0$ [8]. This condition becomes $-l < 0$ in the limit $\sigma \to 0$ since the pulse energy grows exponentially and thus $g(|u|) \to 0$. This behavior appears in our asymptotic solution. As illustrated in Fig. 3, the pulse envelope $|a_0(\tau)|$ decays exponentially as $|\tau| \to \infty$, with a decay rate that becomes infinite as $\sigma \to 0$. As a consequence, the terms proportional to $|a_0|^2$ and $|a_0|^4$ in Eq. (11) become negligible, and Eq. (10) becomes

$$\sigma\frac{\partial \Delta a}{\partial z} = -\frac{l}{2}\sigma\Delta a + \frac{\sigma^{1/2}}{C_g}\frac{g_0}{4\omega_g^2}\Delta a'' - i\left(1 + \frac{\sigma^{1/2}}{C_g}\right)\left(\frac{\beta''}{2}\Delta a'' + \psi_0\Delta a\right). \tag{12}$$

In the Fourier domain, Eq. (12) becomes

$$\frac{\partial \Delta\tilde{a}}{\partial z} = \lambda_c(\omega)\Delta\tilde{a}, \tag{13}$$

where $\Delta\tilde{a}(\omega)$ is the Fourier transform of $\Delta a(\tau)$ and

$$\mathrm{Re}\{\lambda_c(\omega)\} = -\left(\frac{l}{2} + \frac{g_0}{4C_g\sigma^{1/2}\omega_g^2}\omega^2\right). \tag{14}$$

Equation (14) implies that the stationary pulse solution is always stable with respect to continuous modes with $l > 0$.

C. Discrete Modes

The discrete modes can be evaluated computationally by performing an eigenanalysis of the Jacobian of Eq. (10). Here, we study the case when $a_0 \neq 0$ and $\sigma \to 0$. The stability of Δa will be dominated by the zero-order terms in powers of σ on the right-hand side of Eq. (10), so that

$$\sigma\frac{\partial \Delta a}{\partial z} = f_{a^*}, \tag{15}$$

where f_a is defined in Eq. (11). We can then determine the stability of the asymptotic stationary solution by analyzing the spectrum of the Jacobian of the system that is given by Eq. (15). Because Δa^* appears in f_a, we must extend Eq. (15) to include the equation for $\partial\Delta a^*/\partial z$ in order to have a complete eigensystem [11], analogous to what is done in soliton perturbation theory. Instead of directly solving for $\partial\Delta a/\partial z$ and $\partial\Delta a/\partial z^*$, it is computationally convenient to let $a_0(\tau) = v_0(\tau) + iw_0(\tau)$. We then use $\Delta v = (\Delta a + \Delta a^*)/2$ and $\Delta w = (\Delta a - \Delta a^*)/(2i)$ to denote the perturbations to v_0 and w_0. Similar to [8], we discretize the system in a computational window $\tau \in [-T_\tau/2, T_\tau/2]$—where $a_0(\pm T_\tau/2) \approx 0$—using N equispaced points $\{\tau = \tau_j, j = 1, 2, \ldots, N\}$. Using Eq. (15), we formulate the extended system and then a linear eigenvalue problem as

$$\frac{\mathrm{d}}{\mathrm{d}z}\begin{bmatrix}\Delta\mathbf{v}\\ \Delta\mathbf{w}\end{bmatrix} = \mathrm{J}\begin{bmatrix}\Delta\mathbf{v}\\ \Delta\mathbf{w}\end{bmatrix} = \lambda\begin{bmatrix}\Delta\mathbf{v}\\ \Delta\mathbf{w}\end{bmatrix}, \tag{16}$$

where the vectors $\Delta\mathbf{v}$ and $\Delta\mathbf{w}$ are defined as $\Delta\mathbf{v}_j = \Delta v(\tau_j)$ and $\Delta\mathbf{w}_j = \Delta w(\tau_j)$, and the Jacobian matrix J is

$$\mathrm{J} = \begin{bmatrix}\mathrm{J}_{11} & \mathrm{J}_{12}\\ \mathrm{J}_{21} & \mathrm{J}_{22}\end{bmatrix}, \tag{17}$$

where the submatrices are defined as

$$\begin{aligned}
\mathrm{J}_{11} &= \delta(3\mathrm{V}_0^2 + \mathrm{W}_0^2) - 2\gamma\mathrm{V}_0\mathrm{W}_0 - 5\mathrm{V}_0^4 - \mathrm{W}_0^4 - 6\mathrm{V}_0^2\mathrm{W}_0^2,\\
\mathrm{J}_{12} &= 4\mathrm{V}_0\mathrm{W}_0\left(\frac{\delta}{2} - \mathrm{V}_0^2 - \mathrm{W}_0^2\right) - \gamma(\mathrm{V}_0^2 + 3\mathrm{W}_0^2) + \frac{\beta''}{2}\mathrm{D}_\tau^2 + \psi,\\
\mathrm{J}_{21} &= 4\mathrm{V}_0\mathrm{W}_0\left(\frac{\delta}{2} - \mathrm{V}_0^2 - \mathrm{W}_0^2\right) + \gamma(3\mathrm{V}_0^2 + \mathrm{W}_0^2) - \frac{\beta''}{2}\mathrm{D}_\tau^2 - \psi,\\
\mathrm{J}_{22} &= \delta(\mathrm{V}_0^2 + 3\mathrm{W}_0^2) + 2\gamma\mathrm{V}_0\mathrm{W}_0 - \mathrm{V}_0^4 - 5\mathrm{W}_0^4 - 6\mathrm{V}_0^2\mathrm{W}_0^2,
\end{aligned} \tag{18}$$

in which D_τ^2 is the second-order differentiation matrix in τ [8], and both V_0 and W_0 are diagonal matrices with $\mathrm{V}_{0,jj} = v_0(\tau_j)$ and $\mathrm{W}_{0,jj} = w_0(\tau_j)$.

We can determine the stability of the asymptotic stationary solution by analyzing the spectrum of the matrix J. First, we find the contribution of f_a, defined in Eq. (11), to the stability of the continuous modes by setting $\mathrm{V}_0 = \mathrm{W}_0 = 0$ in Eq. (17). When evaluated in the frequency domain, we have

$$\lambda(\omega) = \pm i|\psi_0 - \beta''\omega^2/2|. \tag{19}$$

The continuous spectrum $\lambda(\omega)$ is purely imaginary, which implies that the dominant balance for Eq. (7), given by f in Eq. (8), does not determine the stability; it only indicates the rate of phase rotation of the continuous modes. This result does not affect the stability condition for the continuous modes that we described earlier. In Fig. 4(a), we show the spectrum of J when $\delta = 0.05$. There are four real discrete eigenvalues, which are similar to the spectrum of the stationary solution for the HME. However, in contrast to the HME, the eigenvalue due to the frequency shift is 0, which occurs because the dominant balance in Eq. (8) corresponds to an unfiltered system—the frequency filter scales with the saturated gain, which vanishes as $\sigma \to 0$.

In Fig. 4(b), we show the spectrum of J when $\delta = 13$. We observe that an extra pair of discrete eigenvalues, λ_e and λ_e^*, now exist on the positive real side of the complex plane, which implies that the system is unstable at this large value of δ. As δ decreases, the real part of λ_e decreases, and both λ_e and λ_e^* approach and eventually become indistinguishable from the continuous spectrum.

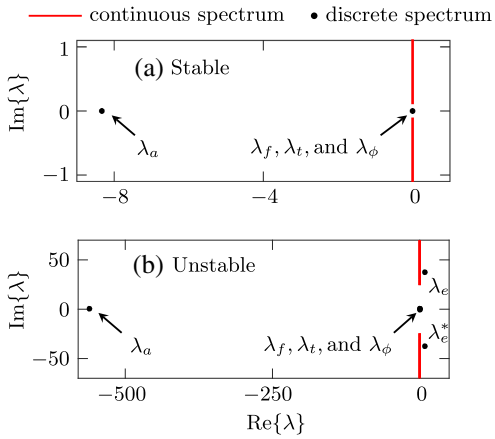

Fig. 4. Spectrum of the Jacobian J in Eq. (17) with (a) $\delta = 0.05$ and (b) $\delta = 13.00$.

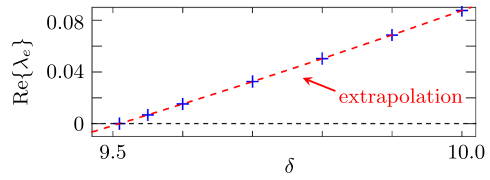

Fig. 5. Variation of the real part of the eigenvalue λ_e, which determines the stability of the asymptotic stationary solution when $\sigma \to 0$.

We use the approach that was described in [8] to calculate the eigenvalues as δ decreases. We show the result in Fig. 5. We find that the real part of these eigenvalues becomes 0 at $\delta \approx 9.5094$. Thus, the asymptotic stationary solution is stable as long as $\delta < 9.5094$, where these two eigenvalues merge into the continuous spectrum and the computation stops. Compared to the stable range of the HME ($0.01 < \delta < 0.0348$) [3], we find that the stability range of CQME is significantly larger. This result is consistent with the stability boundary that we have found in cases with small but nonzero values of σ in [8].

5. DISCUSSION

The stable self-similar solution that we have found in this paper sheds further light on the dynamical structure of the CQME [3,8]. We have found in [8] that, in contrast to the HME where there is only one stable solution, two stable equilibrium pulse solutions can coexist in a region of the parameter space. When $\sigma \to 0$, the low-amplitude solution tends to the stable solution of the HME, where an analytical expression is available, as long as δ is below the HME's stability limit. In this paper, we prove that the high-amplitude solution remains stable as $\sigma \to 0$, although the pulse energy increases and the pulse duration decreases. More significantly, our results show that stabilization of the laser system is achieved by a balance between the cubic and the quintic nonlinearity instead of the saturated gain and linear loss, which is the physical reason that the CQME has a much larger region of stability than does the HME even when the quintic term is small. The stability can still be affected by other system parameters, particularly the group velocity dispersion β''.

In a very large range of δ, when the quintic coefficient disappears, i.e., $\sigma \to 0$, the energy of the high-amplitude solution becomes increasingly large. This behavior is consistent with the way in which unstable solutions of the HME evolve when δ is above the instability threshold ($\delta > 0.0348$). The propagating pulse becomes increasingly narrow and energetic, and it eventually blows up. However, a quintic nonlinearity—no matter how small—is always present in any real laser system, and this quintic nonlinearity will put a halt to the continued growth of the pulse energy. The blowing-up of the propagating pulse that is predicted by the HME [3] has only been observed experimentally in dispersion-managed lasers [18] but not in soliton lasers with anomalous dispersion. Our results provide a theoretical explanation. Such physical insights suggest that the CQME intrinsically provides a better qualitative approximation to practical modelocked lasers than does the HME.

Our results suggest a possible path toward obtaining high-energy and ultrashort laser pulses. The balance of the higher-order nonlinear terms stabilizes these high-energy solutions, so that such solutions can be accessed by decreasing the quintic nonlinearity while keeping the cubic nonlinearity fixed. This result can be achieved in principle by adjusting the parameters of the saturable absorber. For example, we mentioned in [9] that, for a laser in which the fast saturable absorber is a two-level system, the cubic–quintic model is described as

$$f_{\mathrm{sa}}(|u|) = \frac{f_0}{P_{\mathrm{ab}}}|u(t)|^2 - \frac{f_0}{P_{\mathrm{ab}}^2}|u(t)|^4 + \cdots, \tag{20}$$

where f_0 is the saturable absorption, and P_{ab} is the saturation power of the absorber. In order to obtain such high-energy and ultrashort laser pulses, one would increase the saturable power P_{ab} while keeping f_0/P_{ab} fixed. This insight may be difficult to apply to real lasers in which the parameters of the saturable absorber typically lie outside the precise control of experimentalist. However, our results demonstrate that there is a strong motivation to better control these parameters.

Funding. Aviation and Missile Research, Development, and Engineering Center (AMRDEC); Defense Advanced Research Projects Agency (DARPA) (W31P4Q-14-1-0002).

Acknowledgment. We thank Valentin Besse and Thomas Carruthers for useful comments.

REFERENCES

1. S. A. Diddams, "The evolving optical frequency comb [invited]," J. Opt. Soc. Am. B **27**, B51–B62 (2010).
2. F. Kärtner, *Few-Cycle Laser Pulse Generation and Its Applications*, Topics in Applied Physics (Springer, 2014).
3. T. Kapitula, J. N. Kutz, and B. Sandstede, "Stability of pulses in the master mode-locking equation," J. Opt. Soc. Am. B **19**, 740–746 (2002).
4. A. Chong, J. Buckley, W. Renninger, and F. Wise, "All-normal-dispersion femtosecond fiber laser," Opt. Express **14**, 10095–10100 (2006).
5. T. Fortier, D. Jones, J. Ye, and S. Cundiff, "Highly phase stable mode-locked lasers," IEEE J. Sel. Top. Quantum Electron. **9**, 1002–1010 (2003).
6. J. M. Soto-Crespo, N. N. Akhmediev, and V. V. Afanasjev, "Stability of the pulse like solutions of the quintic complex Ginzburg–Landau equation," J. Opt. Soc. Am. B **13**, 1439–1449 (1996).
7. W. H. Renninger, A. Chong, and F. W. Wise, "Dissipative solitons in normal-dispersion fiber lasers," Phys. Rev. A **77**, 023814 (2008).

8. S. Wang, A. Docherty, B. S. Marks, and C. R. Menyuk, "Boundary tracking algorithms for determining the stability of mode-locked pulses," J. Opt. Soc. Am. B **31**, 2914–2930 (2014).
9. S. Wang, B. S. Marks, and C. R. Menyuk, "Comparison of models of fast saturable absorption in passively modelocked lasers," Opt. Express **24**, 20228–20244 (2016).
10. N. N. Akhmediev, J. M. Soto-Crespo, and P. Grelu, "Roadmap to ultra-short record high-energy pulses out of laser oscillators," Phys. Lett. A **372**, 3124–3128 (2008).
11. C. R. Menyuk and S. Wang, "Spectral methods for determining the stability and noise performance of passively modelocked lasers," Nanophotonics **5**, 332–350 (2016).
12. G. Barenblatt, *Scaling, Self-similarity, and Intermediate Asymptotics: Dimensional Analysis and Intermediate Asymptotics*, Cambridge Texts in Applied Mathematics (Cambridge University, 1996).
13. S. Wang and C. R. Menyuk, "Computational methods for determining the stability of pulses in passively modelocked laser systems," in *IEEE Photonics Conference* (2013), pp. 392–393.
14. C. Bao, W. Chang, C. Yang, N. Akhmediev, and S. T. Cundiff, "Observation of coexisting dissipative solitons in a mode-locked fiber laser," Phys. Rev. Lett. **115**, 253903 (2015).
15. V. V. Afanasjev, "Soliton singularity in the system with nonlinear gain," Opt. Lett. **20**, 704–706 (1995).
16. H. A. Haus and A. Mecozzi, "Noise of mode-locked lasers," IEEE J. Quantum Electron. **29**, 983–996 (1993).
17. D. J. Kaup, "Perturbation theory for solitons in optical fibers," Phys. Rev. A **42**, 5689–5694 (1990).
18. S. T. Cundiff, J. M. Soto-Crespo, and N. Akhmediev, "Experimental evidence for soliton explosions," Phys. Rev. Lett. **88**, 073903 (2002).